THE JOURNAL OF PHYSICAL CHEMISTRY B

Article

pubs.acs.org/JPCB

Electron-Induced Degradation of 8-Bromo-2′-deoxyadenosine 3′,5′-Diphosphate, a DNA Radiosensitizing Nucleotide

Lidia Chomicz,[†] Jerzy Leszczynski,[‡] and Janusz Rak*[,†]

[†]Department of Chemistry, University of Gdańsk, Sobieskiego 18, 80-952 Gdańsk, Poland

[‡]Interdisciplinary Nanotoxicity Center, Jackson State University, Jackson, Mississippi, 39217, United States

ABSTRACT: The phosphodiester bond cleavage in 8-bromo-2′-deoxyadenosine 3′,5′-diphosphate (BrdADP), as a model of electron induced single strand break (SSB) in labeled DNA, was investigated at the B3LYP/6-31++G(d,p) level of theory both in the gas phase and in water solution. Barrier-free and highly exergonic, especially in water solution (−2.83 eV), release of the bromide anion due to electron attachment confirms radiosensitizing properties of 8-bromoadenine. Thermodynamically (−19 kcal/mol) and kinetically (barrier of 10−13 kcal/mol) feasible hydrogen atom transfer from the C3′ or C5′ sites of the deoxyribose moiety to the C8 center of adenine radical is followed by a relatively low (14−18 kcal/mol) activation barrier O−P bond cleavage at either the 3′- or the 5′-site. The C5′ radical may also stabilize via the formation of 5′,8-cycloadenosine. The latter process has favorable thermodynamic and kinetic characteristics, which makes the O−P bond breakage at the 5′-site highly unlikely. Thus, the O−P cleavage reaction, being an equivalent of SSB in DNA labeled with 8-bromoadenine, should lead to the formation of cyclic ketone, which if identified in a radiolytic experiment, would confirm the mechanism proposed in the current study.

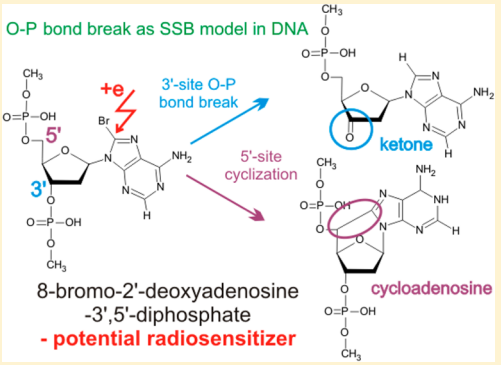

I. INTRODUCTION

DNA is the most important target as concerns cell killing by ionizing radiation (IR). Indeed with eukaryotic cells that contain their DNA in the nucleus, little lethal damage is observed as long as IR is absorbed by membrane or cytoplasm. However, there is a dramatic increase of cellular death as soon as ionizing radiation reaches the nucleus.[1] The observation of a significant amount of nonscavengable DNA damage, even under high concentration of hydroxyl radical scavengers, suggested that direct action of ionizing radiation was responsible for the damage.[2] This, however, remains in contradiction to the fact that the yields of single strand breaks (SSBs) and double strand breaks (DSBs) induced by γ-photons are 3 orders of magnitude larger for aqueous solution than for dry DNA.[3] Thus, the main mechanism by which IR induces cell killing seems to be related to DNA damage by water radiolysis products, and hydrogen and hydroxyl radicals, as well as solvated electrons, are the most abundant among such products.[4,5]

Cancer cells usually suffer from hypoxia, and it has been demonstrated that well-oxygenated cells are more radiosensitive than hypoxic ones, with oxygen enhancement ratios typically between 2.5 and 3.0.[6] Moreover, efficient repair mechanisms in cells further lessen the therapeutic effects of γ-ray/X-ray radiation.[7] The mentioned above facts call for introduction of radiosensitizers, i.e., substances that sensitize cells to radiation, in order to increase the efficiency of any radiotherapy.

Studies with scavenger molecules indicate that almost all of the indirect damage to DNA is due to attack by the highly reactive hydroxyl radicals ($OH^{\bullet}$). Furthermore, it seems that the reducing counterparts of $OH^{\bullet}$, i.e., hydrated electrons, although generated by IR in a yield similar to that of hydroxyl radicals, are unlike presolvated electrons,[8,9] ineffective, especially at inducing DNA strand breaks.[10] The low reactivity of solvated electrons toward DNA may be comprehended by invoking the recent review of Domcke et al. who mention that under the ambient conditions the equilibrated solvated electron is bound by ∼3.4 eV in water.[11] On the other hand, the adiabatic electron affinities of thymine and cytosine incorporated in DNA were calculated to be only around 2 eV.[12,13] Hence, the unfavorable thermodynamic barrier of ∼1.4 eV probably prevents a transfer of hydrated electron to the DNA molecule. This situation may, however, change dramatically provided the modified nucleosides of a sufficient electron affinity are incorporated into cellular DNA. Additionally, in order to be effective radiosensitizers, such nucleosides have to be easily decomposed because of electron attachment, leaving reactive radicals in DNA that in secondary steps may produce strand breaks.

Since the Zamenhof[14] and Greer[15] discovery of photosensitizing capabilities of 5-bromo-2′-deoxyuridine (5-BrdU) toward the *E. coli* cells, halogenated pyrimidines have also been recognized as radiosensitizing agents with potential clinical applications,[16−18] and they continue to be the subject of

Received: March 5, 2013
Revised: June 4, 2013
Published: June 26, 2013

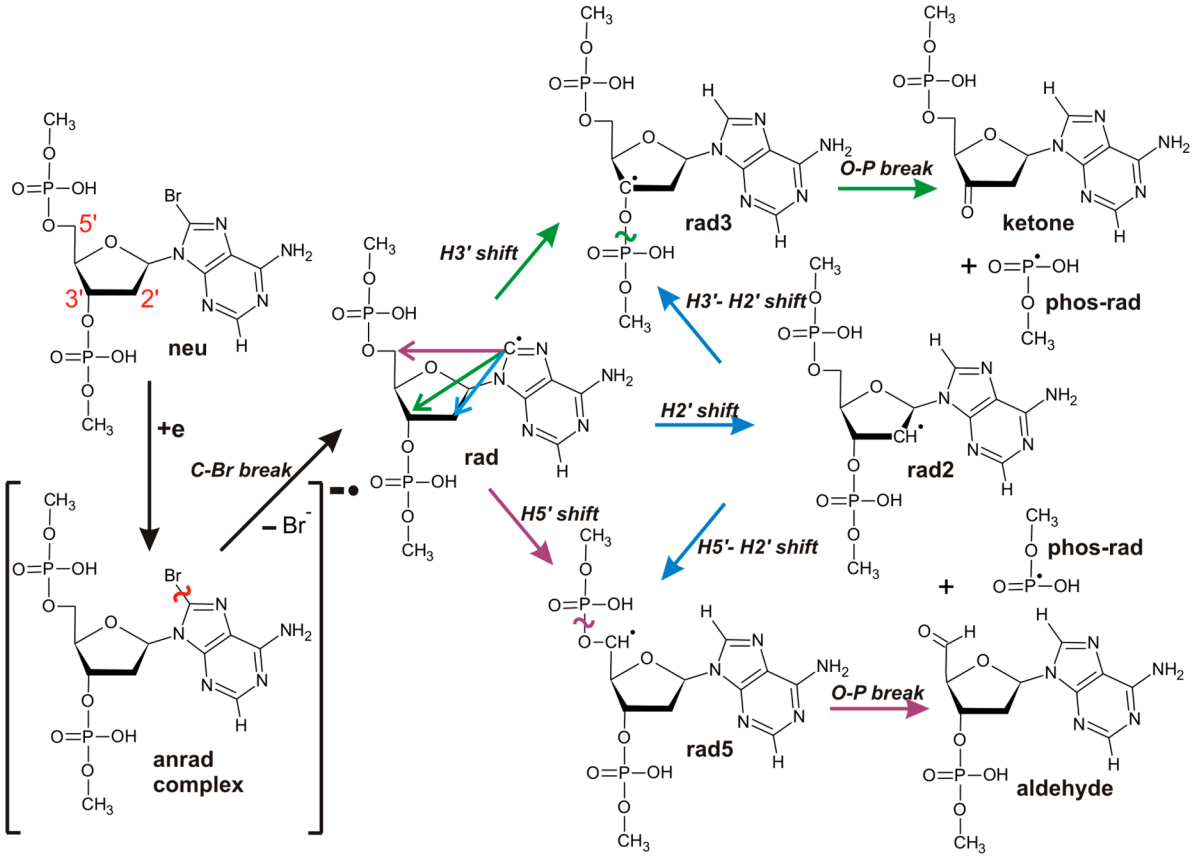

Figure 1. Electron induced BrdADP degradation mechanism.

experiments with cancer cells[19−21] and model DNA fragments.[22−24] Moreover, in the past 10−15 years a renewed interest in the halogenated uridine analogues (5-BrdU and 5-IdU) as radiosensitizing agents for poorly radioresponsive human cancers can be noted.[25]

It is believed that interactions with solvated electrons are responsible for radiosensitizing properties of halogenated uracils (Hal-Us) incorporated in DNA. Because of increased electron affinity of Hal-Us compared to native nucleobases, they can bind the solvated electron, forming primary anions. These unstable species then undergo a rapid halide anion elimination, yielding nearly quantitatively the highly reactive uridine-5-yl radical[26] that in subsequent secondary steps leads to DNA damage.

The sensitivity toward electrons of other halogenated nucleosides, such as 5-bromo-2′-deoxycytidine, 8-bromo-2′-deoxyadenosine, and 8-bromo-2′-deoxyguanosine, both isolated and incorporated into DNA, has also been studied in the past,[27−34] although such studies are scarce compared to those devoted to radiosensitizing properties of halogenated uracils/uridines. Our own B3LYP/6-31++G(d,p) level of computational studies on electron capture by four brominated nucleobases (BrNBs) demonstrate that the overall thermodynamic stimulus for the process starting with the neutral BrNB and ending with the isolated bromide anion and the NB$^{\bullet}$ radical is close to 3 eV in water and similar for all studied BrNBs, which suggests the possibility of binding solvated electrons, as well as their comparable radiosensitizing capabilities.[35] Stimulated by the above-mentioned results, we compared very recently[36,37] low energy electron stimulated desorption (ESD) of anions from thin films of native and brominated single stranded oligonucleotide trimers. These studies demonstrated that their radiosensitivity is due to release of the bromide anion, which is concurrently one of the main degradation paths of the brominated species.[35] Moreover, the HPLC analysis of the products of irradiation with 10 eV electrons showed that the labeled oligonucleotides are 2−4 times more sensitive to LEEs than the native ones.[35]

In the current computational work we study, at the DFT level, electron attachment to a model nucleotide of bromoadenosine, i.e., to 8-bromo-2′-deoxyadenosine 3′,5′-diphosphate (BrdADP), followed by secondary reactions that lead to an equivalent of single strand break. We demonstrate that electron attachment to the studied nucleotide triggers barrier-free release of the bromide anion. The radical occurring as a consequence of this primary process may stabilize itself via low-barrier hydrogen atom transfer from the sugar moiety to the base which eventually leads to the dissociation of the O−P bond. In addition, the formation of 5′,8-cycloadenosine, a well-known damage related to adenosine radical,[38] that may interfere with the O−P breakage is addressed. Thus, for the first time we propose a strand break mechanism that can be operative in exposed-to-ionizing-radiation aqueous solutions of DNA labeled with 8-bromoadenine.

II. COMPUTATIONAL METHODS

We applied the density functional theory method with Becke's three-parameter hybrid functional (B3LYP)[39] and the 6-31++G(d,p) basis set[40] to the gas phase calculations and additionally the polarizable continuum model (PCM)[41] to the aqueous solution. The same methodology has been

dx.doi.org/10.1021/jp4022689 | J. Phys. Chem. B 2013, 117, 8681−8688

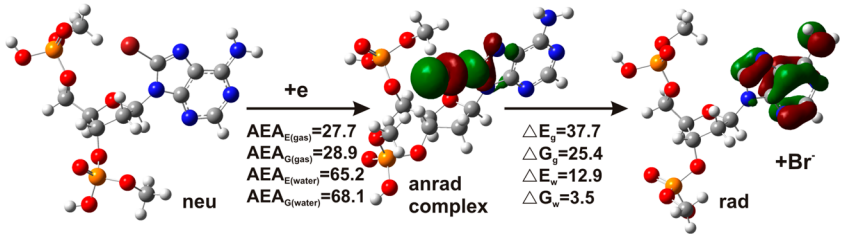

Figure 2. Bromide anion release after electron attachment. Stationary geometries and singly occupied molecular orbitals (SOMOs, for radicals only), along with electron affinities (AEA) and thermodynamic characteristics for anrad complex dissociation, calculated at the B3LYP/6-31++G(d,p) level. All values are in kcal/mol. Orbitals are plotted with a contour value of 0.05 $(bohr)^{-3/2}$. Gas phase data are denoted with "g", while water solution data are denoted with "w".

previously used to describe the dissociation of brominated nucleobases induced by electron attachment.[33]

The energies of particular reaction steps (ΔE) were calculated as the differences between the electronic energies of substrates and products, while the Gibbs free energies of these steps (ΔG) were ΔE values corrected for zero-point vibration terms, thermal contributions to energy, the pV term, and the entropy term. These terms were calculated in the rigid rotor−harmonic oscillator approximation at T = 298 K and p = 1 atm. In order to calculate ΔG for the solvated systems, the same correction terms were applied to the solute as were used for calculating the gas-phase free energies.[42]

The adiabatic electron affinity, AEA_E, is defined as the difference in electronic energies of the neutral entity and the given anion radical complex at their corresponding fully relaxed structures. Moreover, the adiabatic electron affinity, calculated using Gibbs free energies of the fully optimized neutral and anion radical complex, is denoted by AEA_G.

All calculations have been carried out with the Gaussian 09[43] code. The images of the molecules were plotted with the GaussView package.[44]

III. RESULTS AND DISCUSSION

In the following we propose a mechanism that explains how single strand break can occur after electron attachment to DNA containing 8-bromoadenine. Two degradation paths of the brominated nucleotide anion, leading via the bromide anion detachment and intranucleotide hydrogen atom transfer to phosphodiester bond breakage with a ketone- or aldehyde-derivative formation, have been considered (see Figure 1).

Model. The brominated purine nucleotide 8-bromo-2′-deoxyadenosine 3′,5′-diphosphate (BrdADP), a potential radiosensitizer,[34,35] was chosen to model an electron induced degradation of the substituted DNA. The starting geometry of the nucleotide was based on the experimental X-ray geometry of adenosine present in the double stranded DNA fragment.[45] Namely, the geometry of BrdADP was extracted from the above-mentioned fragment by cutting the O−P bonds connecting adenosine to its 5′ and 3′ nucleotide neighbors. Then the unsaturated bonds were filled with the methyl groups and the negative charge of phosphates was neutralized by protons that were attached to phosphates' oxygens (under physiological pH the negative charge of phosphate is neutralized by a sodium/potassium cation). First, the usage of neutralizing protons simplifies the calculations. Second, it was demonstrated that the AEAs of pyrimidine nucleotides are almost independent of their ionization state.[46,47] Therefore, protonation of phosphates only marginally influences the electrophilic properties of the studied system. Finally, the hydrogen atom bound to the C8 of adenine has been substituted with bromine and the initial C8−Br distance was set to 1.9 Å, i.e., close to its equilibrium B3LYP/6-31++G(d,p) value calculated for 9-methyl-8-bromodenine[33] (see the neu structure in Figure 1). The B3LYP optimization of the geometry obtained in the above-described manner led to a nucleotide conformation that was very similar to the starting one. Thus, it suggests that the chosen model properly accounts for the conformational constraints present in double-stranded DNA.

First Step: Electron Induced Bromide Anion Release. Electron attachment to the neutral form of BrdADP (neu; see Figures 1 and 2) causes an immediate, barrier free C−Br bond break that ends up at the specific anion radical complex (anrad complex, see Figures 1 and 2), both in the gas phase and in water solution. A similar barrier-free process has been predicted recently[33] for the 9-methyl-8-bromoadenine anion which shows that the presence of DNA backbone does not introduce a barrier for the dissociation of the C8−Br bond. Note that although the geometry relaxation of the anion leads to anrad complex, the vertical (neutral geometry) attachment of electron to BrdADP results in a typical π^* radical anion.

The AEA value calculated for anrad complex proves its high adiabatical stability, especially in an aqueous solution (see Figure 2). The AEA of 2.83 eV calculated for BrdADP in water is 0.19 eV larger than that obtained recently, at the same level of theory, for 9-methyl-8-bromoadenine.[33] It is worth emphasizing that a similar increase in electron affinity was predicted for unsubstituted adenine as the AEA calculated at the B3LYP/6-31+G(d,p) level and the PCM model of water amounts to 1.44 eV for the base while it is equal to 1.59 eV for 2′-deoxyadenine 3′,5′-diphosphate (dADP).[12] Thus, the 0.15 eV difference between the respective AEAs in favor of unsubstitued diphosphate is both qualitatively and quantitatively similar to that (0.19 eV) resulting from the AEAs of the brominated adenine and its nucleotide. This analogy demonstrates that similar effects are responsible for the electrophilic properties of adenine and bromoadenine based systems and the main difference between them lies in much stronger stabilization of the excess electron by the brominated analogues, cf. the AEA of 2.83 eV for BrdADP with the AEA of 1.59 eV for dADP. Such a large AEA value for the brominated adenine diphosphate accounts well for the radiosensitizing properties of bromoadenine incorporated in DNA. Indeed, this value falls in the range of energies characteristic for equilibrated hydrated electron, i.e., −2.5 to −4 eV with a maximum at −3.4 eV, as was measured in charge-transfer-to-solvent experiments.[48] It is worth noting that in an aqueous solution the AEAs of native nucleotides are below 2 eV[12] which explains the

dx.doi.org/10.1021/jp4022689 | J. Phys. Chem. B 2013, 117, 8681−8688

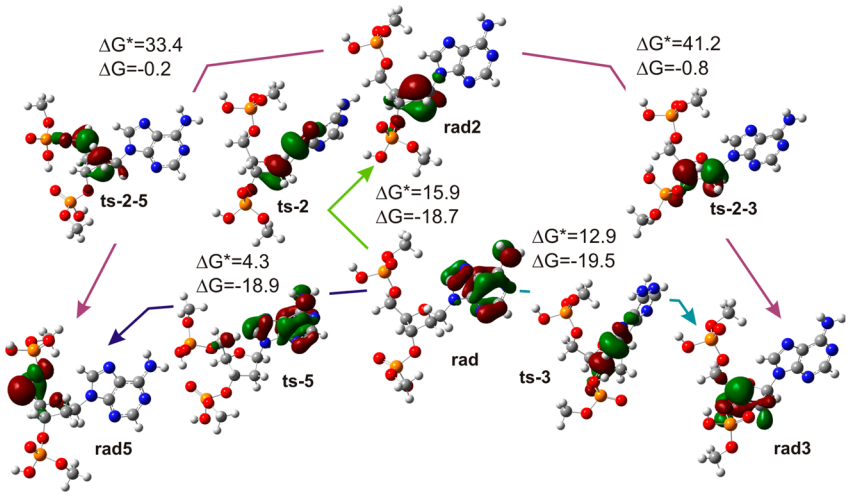

Figure 3. Intranucleotide radicals transformations: stationary geometries and SOMO orbitals, plotted with a contour value of 0.05 $(bohr)^{-3/2}$. Energetic characteristics are given in kcal/mol for an aqueous solution.

resistance of pristine DNA to damage induced by hydrated electrons.

A complete separation of the adenine localized radical and bromide anion (dissociation of anrad complex, see the second reaction in Figure 2) is thermodynamically highly unfavorable in the gas phase (ΔG_g = 25.5 kcal/mol), while it becomes much more likely in a water environment (ΔG_w = 3.5 kcal/mol). Electron induced debromination is a crucial step for the studied mechanism, as it generates a reactive adenine nucleotide radical (rad) that stabilizes in two consecutive steps leading eventually to the O−P bond cleavage, i.e., to single strand break if the considered nucleotide is a part of DNA. It is worth noting that such breakage mechanism has only a chance to occur if intramolecular hydrogen transfer processes within DNA are substantially faster than intermolecular quenching of adenosine radical formed via the electron induced debromination. Indeed, in the experiments on excess electron transfer in double-stranded model duplexes labeled with brominated uridine, adenosine, and guanosine only debromination of the bromo derivatives due to the reaction of respective nucleoside radicals with additives was observed.[33,34]

Intranucleotide Hydrogen Atom Transfer. Three ways of stabilization of the rad radical, with unpaired electron localized on the purine ring, were considered (see Figures 1 and 3). Namely, rad could be stabilized by hydrogen atom transfer from its own deoxyribose moiety at the C2′, C3′, and C5′ positions (see Figure 4). The kinetic and thermodynamic data representing stimuli for these transformations are gathered in Table 1.

Counterintuitively, despite the shortest C8−H distance (2.73 Å; see Figure 4), the H2′ atom shift, with the highest kinetic barrier and the lowest thermodynamic stimulus (see Table 1), is the least favorable way for rad stabilization. These findings seem to be corroborated by the literature data that indicate that the 2′-position of deoxyribose is not a commonly invoked abstraction site in DNA.[49] Moreover, the second most efficient reaction, i.e., liberation of adenine, observed during the radiolysis of aqueous solutions of 8-bromoadenosine (8-BrA) containing *tert*-butanol (*t*-BuOH), was ascribed to the formation of the C2′ radical forming as a result of radical translocation from the C8 site of the adenine moiety.[50] Unlike in 8-BrA solutions, free adenine assayed in radiolyzed 8-bromo-

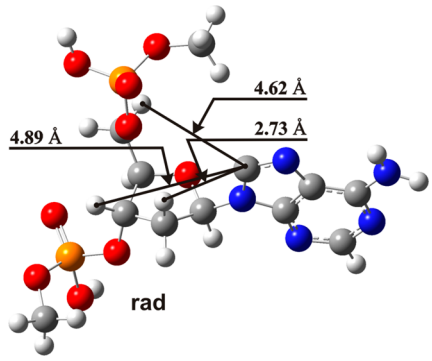

Figure 4. Rad stationary geometry with the values of molecular distances between the centers involved in the hydrogen atom transfer reactions.

2′-deoxyadenosine (8-BrdA) constitutes only a minor degradation pathway[29,30] and probably forms in reactions between the *t*-BuOH radical and sugar moiety.[30] The results of DFT studies carried out by the Chatgilialoglu group[50] remain in accordance with our findings (see Table 1) and account well for the above-described difference in the radiolytic behavior of 8-BrA and 8-BrdA. Namely, radical translocation to the C2′ site proceeds with the activation barrier of only 10 kcal/mol in 8-BrA while the analogous process concerning 8-BrdA is associated with a barrier height of as much as 16 kcal/mol.[50]

The most likely hydrogen transfer is the H5′ shift, whose activation barrier amounts to only 4.0 and 4.3 kcal/mol in the free enthalpy scale for the gas phase and aqueous solution, respectively (see Table 1). It again remains in agreement with the literature data that indicate that the C5′ radical is most abundant in radiolyzed solutions containing 8-BrdA.[29] However, it should be borne in mind that those barriers are underestimated because of the sugar−phosphate backbone bending that accompanies the formation of the rad5 transition state structure (compare ts-5 with ts-2 and ts-3 in Figure 3). Indeed, because of the conformational constraints present in double-stranded DNA, a geometry corresponding to the ts-5 structure cannot be formed in the biopolymer. On the other hand, the hydrogen bond between the phosphates (see ts-5 in Figure 3), improbable in native DNA, increases the stability of ts-5, thus leading to underestimation of the calculated barrier.

dx.doi.org/10.1021/jp4022689 | J. Phys. Chem. B 2013, 117, 8681−8688

Table 1. Thermodynamic (ΔE and ΔG) and Kinetic (ΔE^* and ΔG^*) Characteristics of Particular Reaction Steps for the BrdADP Degradation Mechanism (see Figure 1)[a]

step	gas phase				aqueous solution			
	ΔE^*	ΔE	ΔG^*	ΔG	ΔE^*	ΔE	ΔG^*	ΔG
Intranucleotide Hydrogen Atom Transfer								
rad → rad2	21.5	−15.7	19.3	−16.2	18.2	−17.1	15.9	−18.7
rad → rad3	15.7	−16.7	15.3	−18.8	14.7	−18.4	12.9	−19.5
rad → rad5	3.7	−17.4	4.0	−17.7	4.6	−18.0	4.3	−18.9
	11.6[b]				10.7[b]			
H Transfer within Deoxyribose								
rad2 → rad3	42.8	−1.0	40.6	−2.5	43.5	−1.3	41.2	−0.8
rad2 → rad5	31.0	−1.7	31.6	−1.5	32.4	−0.9	33.4	−0.2
	38.9[b]				39.0[b]			
O−P Bond Break								
rad3 → ketone-rad	7.7	−2.9	11.4	−2.8	12.3	0.3	14.4	−0.9
rad5 → aldehyde-rad	19.4	−2.5	18.0	−3.4	19.1	8.9	18.5	4.4
Complex Dissociation								
ketone-rad → ketone + phos-rad		14.3		3.9		10.7		−1.7
aldehyde-rad → aldehyde + phos-rad		23.6		9.1		7.8		−1.6
Cycloadenosine Formation								
rad5 → cycloadenosine	13.2	−9.1	16.5	−4.4	11.7	−10.3	14.0	−6.3
Total Driving Force for the Formation of Damage								
rad → ketone + phos-rad		−5.4		−17.6		−7.5		−22.2
rad → aldehyde + phos-rad		3.7		−12.0		−1.3		−16.0
rad → cycloadenosine		−26.1		−22.1		−28.3		−25.1

[a]All values in kcal/mol. [b]Activation barriers calculated for the corresponding transition state structure with sugar−phosphate backbone frozen in dsDNA conformation.

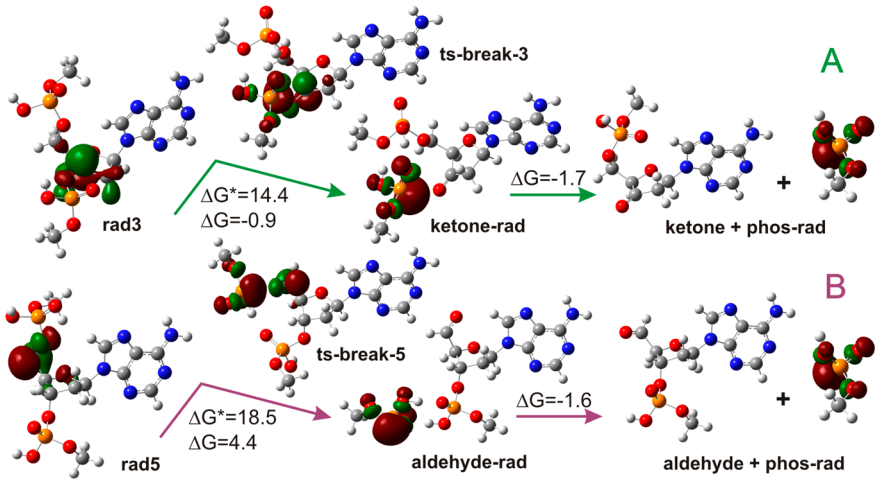

Figure 5. Phosphodiester bond breakage paths, leading to ketone (path A) or aldehyde (path B) derivative product: stationary geometries and SOMO orbitals, plotted with a contour value of 0.05 $(\text{bohr})^{-3/2}$. Energetic characteristics are given in kcal/mol for an aqueous solution.

In order to estimate the magnitude of this effect, we recalculated the ts-5 structure with its sugar−phosphate backbone frozen at rad's conformation (recall that the rad geometry closely resembles the crystallographic conformation of 2′-deoxyadenosine in dsDNA). The constrained geometry optimizations of the ts-5 structure result in 7.9 and 6.1 kcal/mol increase of the energy of ts-5, which translates into the activation barrier of 11.6 and 10.7 kcal/mol in the gas phase and aqueous solution, respectively. Although such corrected barrier for the rad → rad5 transformation is still the lowest one among the barriers calculated for hydrogen atom shift, one can conclude, based on the values gathered in Table 1, that the rad → rad5 and rad → rad3 elemental reactions may be quite competitive.

As rad2 is unable to be stabilized through a direct single strand break, conversions of this species into the rad3 and rad5 radicals, capable of transforming into the final degradation products, i.e. into the SSB analogues (see Figure 1), were considered. The kinetic barriers calculated for these processes are ∼40 kcal/mol (see Table 1; note that ts-2−5 is stabilized by the internal hydrogen bond (see Figure 3). Such a structure is not allowed in dsDNA (see the above discussion for ts-5)), which suggests that they are highly improbable. This finding seems to be confirmed by the observation that in those strand scission reactions that imply involvement of the C2′-hydrogen abstraction, the 2′-deoxyribosyl radical is stabilized via a reaction with molecular oxygen to form a peroxide[51] rather than in an internal rearrangement process.

dx.doi.org/10.1021/jp4022689 | J. Phys. Chem. B 2013, 117, 8681−8688

O−P Bond Breakage and Cyclized Aminyl Radical Formation. The rad radical is transformed into rad3 or rad5 by the respective hydrogen atoms transfer, and the latter species may undergo a phosphodiester bond breakage. The O−P bond break in rad3 leads to a ketone radical complex (ketone-rad, path A; see Figure 5), while the cleavage of the analogous bond in rad5 produces an aldehyde radical complex (aldehyde-rad, path B; see Figure 5).

One may ask why the O−P rather than C*X*−O (where *X* = 3′ or 5′) bond cleavage is postulated in the current work. Although studies on LEE-induced damage in model oligonucleotides[52,53] suggested the cleavage of the O−P bond, this was considered to be only a minor route to the formation of single strand breaks in DNA. Note, however, that the attachment of electron to BrdADP leads, after release of the bromide anion (see Figure 2), to rad3 or rad5 which is a neutral rather than an anionic radical (the radical anions of nucleotides do undergo SSB via the C*X*−O bond scission[13]). This is why elongation of the C*X*−O bond in rad3 or rad5, leading to its homolytic dissociation, results in a high-energy open-shell singlet (at least 60 kcal/mol above the energy of substrate[54]), localized on the sugar, and a doublet localized on the phosphate unit. On the other hand, O−P bond dissociation yields a stable carbonyl group instead of the above-mentioned high-energy open-shell singlet together with a phosphoryl radical (phos-rad; see Figure 1). Depending on which O−P bond is broken, from the 3′- or 5′-side, the carbonyl group becomes part of the cyclic ketone or aldehyde (see Figures 2 and 4). Thermodynamically, both paths are comparable, especially in the gas phase, but taking into account also activation barriers, ketone-rad formation seems to be more likely (see Table 1). The very last step of the considered mechanism represents complete separation of the respective complexes (see Figure 5). This separation is thermodynamically favorable only in the aqueous solution (negative free enthalpy change) (see Table 1). In summary, in water both the thermodynamics and kinetics favor the degradation route leading to the ketone derivative (see Figure 5A). This conclusion is confirmed as well by the total thermodynamic stimuli calculated for the transformation of rad into completely separated products (see Table 1). Indeed, ΔG of −17.6 and −22.2 kcal/mol for rad → ketone + phos-rad, and −12.0 and −16.0 kcal/mol for rad → aldehyde + phos-rad were calculated in the gas phase and water solution, respectively (see Table 1).

Another argument, confirming strongly the latter conclusion, i.e., that the ketone derivative should be the main product of the O−P cleavage, is a competitive transformation of rad5 into cycloadenosine (cycloA). Indeed, radiolysis of solutions containing 8-bromo-2′-deoxyadenosine as well as DNA labeled with 8-BrdA leads to the efficient formation of cycloadenosine lesion.[38] Out of four possible conformations leading to stereochemically different products we chose that which in the case of 8-BrdA is characterized by the smallest activation barrier.[29] In Figure 6 the respective stationary points along with the free energy and activation energy are depicted while the complete thermodynamic and kinetic characteristics are gathered in Table 1. Comparing energetic characteristics for the formation of the cyclized aminyl radical (ΔG = −6.3 and ΔG^* = 14.0 kcal/mol; see Table 1) with those for the breakage of the O−P bond from the 5′-side (ΔG = 4.4 and ΔG^* = 18.5 kcal/mol; see Table 1) as well as the total driving force leading from rad to cycloadenosine with that leading to aldehyde (see Table 1), one can draw a conclusion that the latter process is completely quenched. Thus, the attachment of solvated electron to 8-BrdA incorporated into DNA may lead to the O−P break (3′-side) resulting in the cyclic ketone derivative and 5′,8-cycloadenosine lesion.

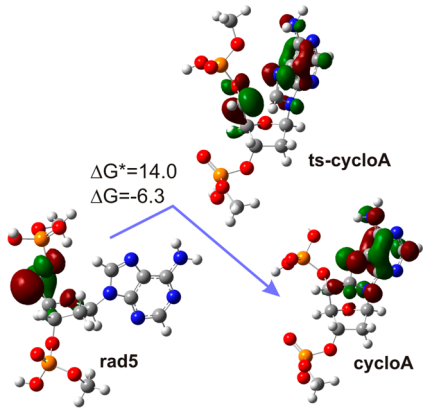

Figure 6. Stationary geometries and SOMO orbitals, plotted with a contour value of 0.05 $(\text{bohr})^{-3/2}$ for cycloadenosine formation. Energetic characteristics are given in kcal/mol for an aqueous solution.

IV. SUMMARY

In the current studies, the electron-attachment induced phosphodiester bond cleavage in 8-bromo-2′-deoxyadenosine 3′,5′-diphosphate has been modeled at the B3LYP/6-31++G(d,p) level both in the gas phase and in aqueous solution. The cleavage of the phosphodiester bond in the studied nucleotide mimics the electron induced single strand break in DNA sensitized to radiolysis with 8-bromoadenine. Our results show unequivocally that the AEA of BrdADP is much larger than that of its native analogue and in an aqueous solution assumes values overlapping the stabilization energies of hydrated electron. This seems to explain well the sensitizing properties of the brominated nucleotide.

An excess electron attachment to BrdADP leads to the barrier-free release of the bromide anion, and the resulting neutral adenine-centered radical may further undergo a sequence of stepwise reactions leading eventually to the phosphodiester bond cleavage that is an equivalent of SSB in DNA. Although a hydrogen atom can be transferred to the C8 site of adenine radical from the C2′, C3′, and C5′ positions of the deoxyribose ring, the calculated kinetic and thermodynamic parameters suggest the abstraction from the C2′ center to be the least probable. Moreover, the role of the C2′ site in the phosphodiester bond cleavage seems to be negligible, since the H5′ or H3′ shifts to the C2′ position, enabling the final dissociation of the nucleotide, are improbable because of their extremely high activation barriers. As opposed to strand breaks induced by electron attachment to unsubstituted DNA, where SSBs are generated as a result of the C*X*−O bond dissociation, SSB in 8-bromoadenine labeled DNA should be associated with the O−P bond cleavage. Depending on which O−P bond is cleaved (from the 3′- or 5′-side), the resulting carbonyl group becomes a part of the cyclic ketone or aldehyde. The calculated thermodynamic and kinetic characteristics suggest that the ketone-type species should constitute the main product in radiolyzed solutions of DNA labeled with 8-bromoadenine. Another argument for the formation of the cyclic ketone exclusively is the fact that because of the efficient way of stabilization of the C5′ radical, i.e., via the formation of cyclized

dx.doi.org/10.1021/jp4022689 | J. Phys. Chem. B 2013, 117, 8681−8688

aminyl radical, the generation of aldehyde is not competitive at all.

An experimental identification of fragments containing cyclic ketone would be a strong argument confirming the electron-induced degradation mechanism proposed in the current work. Therefore, radiolytic studies on DNA labeled with 8-bromoadenine that employ the enzymatic digestion of damaged DNA and LC/MS identification of degradation products are under way in our laboratory.

AUTHOR INFORMATION

Corresponding Author

*E-mail: janusz@raptor.chem.univ.gda.pl.

Notes

The authors declare no competing financial interest.

ACKNOWLEDGMENTS

This work was supported by the Polish National Science Center (NCN) under Grant No. N N204 156040 (J.R.) and by NFS CREST Interdisciplinary Nanotoxicity Center NSF-CREST Grant No. HRD-0833178 (J.L.). Calculations have been carried out at Wroclaw Center for Networking and Supercomputing (http://www.wcss.wroc.pl), Grant No. 209 (L.C.).

REFERENCES

(1) Warters, R. L.; Hofer, K. G.; Harris, C. R.; Smith, J. M. Radionuclide Toxicity in Cultured Mammalian Cells. Elucidation of the Primary Site for Radiation Induced Division Delay. *Curr. Top. Radiat. Res.* **1978**, *12*, 389−407.

(2) deLara, C. M.; Jenner, T. J.; Townsend, K. M. S.; Marsden, S. J.; O'Neill, P. The Effect of Dimethyl Sulfoxide on the Induction Of DNA Double-Strand Breaks in V79-4 Mammalian Cells by Alpha Particles. *Radiat. Res.* **1995**, *144*, 43−49.

(3) Ito, T.; Baker, S. C.; Stickley, C. D.; Peak, J. G.; Peak, M. J. Dependence of the Yield of Strand Breaks Induced by γ-Rays in DNA on the Physical Conditions of Exposure: Water Content and Temperature. *Int. J. Radiat. Biol.* **1993**, *63*, 289−296.

(4) von Sonntag, C. *The Chemical Basis of Radiation Biology*; Taylor and Francis: London, U.K., 1987.

(5) Ershov, B. G.; Gordeev, A. V. A Model for Radiolysis of Water and Aqueous Solutions of H_2, H_2O_2 and O_2. *Radiat. Phys. Chem.* **2008**, *77*, 928−935.

(6) Daşu, A.; Denekamp, J. New Insights into Factors Influencing the Clinically Relevant Oxygen Enhancement Ratio. *Radiother. Oncol.* **1998**, *46*, 269−277.

(7) Joiner, M.; van der Kogel, A. *Basic Clinical Radiobiology*, 4th ed.; Hodder Arnold: London, U.K., 2009.

(8) Wang, C.-R.; Nguyen, J.; Lu, Q.-B. Bond Breaks of Nucleotides by Dissociative Electron Transfer of Nonequilibrium Prehydrated Electrons: A New Molecular Mechanism for Reductive DNA Damage. *J. Am. Chem. Soc.* **2009**, *131*, 11320−11322.

(9) Nguyen, J.; Y Ma, Y.; T Luo, T.; Bristow, R. G.; Jaffray, D. A.; Lu, Q.-B. Direct Observation of Ultrafast-Electron-Transfer Reactions Unravels High Effectiveness of Reductive DNA Damage. *Proc. Natl. Acad. Sci. U.S.A.* **2011**, *108*, 11778−11783.

(10) Michael, B. D.; O'Neill, P. A Sting in the Tail of Electron Tracks. *Science* **2000**, *287*, 1603−1604.

(11) Abel, B.; Buck, U.; Sobolewski, A. L.; Domcke, W. On the Nature and Signatures of the Solvated Electron in Water. *Phys. Chem. Chem. Phys.* **2012**, *14*, 22−34.

(12) Gu, J.; Xie, Y.; Schaefer, H. F., III. Electron Attachment to DNA Single Strands: Gas Phase and Aqueous Solution. *Nucleic Acids Res.* **2007**, *35*, 5165−5172.

(13) Gu, J.; Leszczynski, J.; Schaefer, H. F., III. Interactions of Electrons with Bare and Hydrated Biomolecules: From Nucleic Acid Bases to DNA Segments. *Chem. Rev.* **2012**, *112*, 5603−5640.

(14) Greer, S.; Zamenhof, S. Effect of 5-Bromouracil in Deoxyribonucleic Acid of *E. Coli* on Sensitivity to Ultraviolet Irradiation. *Abstracts of Papers*, 131st National Meeting of the American Chemical Society, Miami Beach, FL, April 7−12, 1957; American Chemical Society: Washington, DC, 1957; p 3C.

(15) Greer, S. Studies on Ultraviolet Irradiation of *Escherichia coli* Containing 5-Bromouracil in Its DNA. *J. Gen. Microbiol.* **1960**, *22*, 618−634.

(16) Djordjevic, B.; Szybalski, W. Genetics of Human Cell Lines. III. Incorporation of 5-Bromo- and 5-Iododeoxyuridine into the Deoxyribonucleic Acid of Human Cells and Its Effect on Radiation Sensitivity. *J. Exp. Med.* **1960**, *112*, 509−531.

(17) Erikson, R. L.; Szybalski, W. Molecular Radiobiology of Human Cell Lines: V. Comparative Radiosensitizing Properties of 5-Halodeoxycytidines and 5-Halodeoxyuridines. *Radiat. Res.* **1963**, *20*, 252−262.

(18) Cramer, J. W.; Prusoff, W. H.; Welch, A. D.; Sartorelli, A. C.; Delamore, I. W.; Von Essen, C. F.; Chang, P. K. Studies on the Biochemical Pharmacology of 5-Iodo-2′-deoxycytidine in Vitro and in Vivo. *Biochem. Pharmacol. (Amsterdam, Neth.)* **1962**, *11*, 761−768.

(19) Brust, D.; Feden, J.; Farnsworth, J.; Amir, C.; Broaddus, W. C.; Valerie, K. Radiosensitization of Rat Glioma with Bromodeoxycytidine and Adenovirus Expressing Herpes Simplex Virus-Thymidine Kinase Delivered by Slow, Rate-Controlled Positive Pressure Infusion. *Cancer Gene Ther.* **2000**, *7*, 778−788.

(20) Dabaja, B. S.; McLaughlin, P.; Ha, C. S.; Pro, B.; Meyers, C. A.; Seabrooke, L. F.; Wilder, R. B.; Kyritsis, A. P.; Preti, H. A.; Yung, W. K.; Levin, V.; Cabanillas, F.; Cox, J. D. Primary Central Nervous System Lymphoma: Phase I Evaluation of Infusional Bromodeoxyuridine with Whole Brain Accelerated Fractionation Radiation Therapy after Chemotherapy. *Cancer* **2003**, *98*, 1021−1028.

(21) Prados, M. D.; Seiferheld, W.; Sandler, H. M.; Buckner, J. C.; Phillips, T.; Schultz, C.; Urtasun, R.; Davis, R.; Gutin, P.; Cascino, T. L.; Greenberg, H. S.; Curran, W. J., Jr. Phase III Randomized Study of Radiotherapy plus Procarbazine, Lomustine, and Vincristine with or without Budr for Treatment of Anaplastic Astrocytoma: Final Report of Rtog 9404. *Int. J. Radiat. Oncol., Biol., Phys.* **2004**, *58*, 1147−1152.

(22) Cecchini, S.; Girouard, S.; Huels, M. A.; Sanche, L.; Hunting, D. J. Single-Strand-Specific Radiosensitization of DNA by Bromodeoxyuridine. *Radiat. Res.* **2004**, *162*, 604−615.

(23) Cecchini, S.; Girouard, S.; Huels, M. A.; Sanche, L.; Hunting, D. J. Interstrand Cross-Links: A New Type of γ-Ray Damage in Bromodeoxyuridine-Substituted DNA. *Biochemistry* **2005**, *44*, 1932−1940.

(24) Dextraze, M.-E.; Wagner, J. R.; Hunting, D. J. 5-Bromodeoxyuridine Radiosensitization: Conformation-Dependent DNA Damage. *Biochemistry* **2007**, *46*, 9089−9097.

(25) Kinsella, T. J. Update on Radiosensitization by Halogenated Thymidine Analogs—Molecular Mechanisms of Drug Processing and Cell Death Signaling: Implications for Future Clinical Trials. *Cancer Biol. Ther* **2008**, *7*, 1567−1569 and references therein.

(26) Li, X.; Sanche, L.; Sevilla, M. D. Dehalogenation of 5-Halouracils after Low Energy Electron Attachment: A Density Functional Theory Investigation. *J. Phys. Chem. A* **2002**, *106*, 11248−11253.

(27) Razskazovskii, Y.; Swarts, S. G.; Falcone, J. M.; Taylor, C.; Sevilla, M. D. Competitive Electron Scavenging by Chemically Modified Pyrimidine Bases in Bromine-Doped DNA: Relative Efficiencies and Relevance to Intrastrand Electron Migration Distances. *J. Phys. Chem. B* **1997**, *101*, 1460−1467.

(28) Flyunt, R.; Bazzanini, R.; Chatgilialoglu, C.; Mulazzani, Q. G. Fate of the 2′-Deoxyadenosin-5′-yl Radical under Anaerobic Conditions. *J. Am. Chem. Soc.* **2000**, *122*, 4225−4226.

(29) Chatgilialoglu, C.; Guerra, M.; Mulazzani, Q. G. Model Studies of DNA C5′ Radicals. Selective Generation and Reactivity of 2′-Deoxyadenosin-5′-yl Radical. *J. Am. Chem. Soc.* **2003**, *125*, 3839−3848.

(30) Boussicault, F.; Kaloudis, P.; Caminal, C.; Mulazzani, Q. G.; Chatgilialoglu, C. The Fate of C5′ Radicals of Purine Nucleosides under Oxidative Conditions. *J. Am. Chem. Soc.* **2008**, *130*, 8377−8385.
(31) Chatgilialoglu, C.; Caminal, C.; Guerra, M.; Mulazzani, Q. G. Tautomers of One-Electron-Oxidized Guanosine. *Angew. Chem., Int. Ed.* **2005**, *44*, 6030−6032.
(32) Chatgilialoglu, C.; Caminal, C.; Altieri, A.; Vougioukalakis, G. C.; Mulazzani, Q. G.; Gimisis, T.; Guerra, M. Tautomerism in the Guanyl Radical. *J. Am. Chem. Soc.* **2006**, *128*, 13796−13805.
(33) Manetto, A.; Breeger, S.; Chatgilialoglu, C.; Carell, T. Complex Sequence Dependence by Excess Electron Transfer through DNA with Different Strength Electron Acceptors. *Angew. Chem., Int. Ed.* **2006**, *45*, 318−321.
(34) Fazio, D.; Trindler, C.; Heil, K.; Chatgilialoglu, C.; Carell, T. Investigation of Excess Electron Transfer in DNA Double-Duplex Systems Allows Estimation of Absolute Excess Electron Transfer and CPD Cleavage Rates. *Chem.—Eur. J.* **2011**, *17*, 206−212.
(35) Chomicz, L.; Rak, J.; Storoniak, P. Electron-Induced Elimination of the Bromide Anion from Brominated Nucleobases. A Computational Study. *J. Phys. Chem. B* **2012**, *116*, 5612−5619.
(36) Polska, K.; Rak, J.; Bass, A. D.; Cloutier, P.; Sanche, L. Electron Stimulated Desorption of Anions from Native and Brominated Single Stranded Oligonucleotide Trimers. *J. Chem. Phys.* **2012**, *136*, 075101.
(37) Park, Y.; Polska, K.; Rak, J.; Wagner, J. R.; Sanche, L. Fundamental Mechanisms of DNA Radiosensitization: Damage Induced by Low-Energy Electrons in Brominated Oligonucleotide Trimers. *J. Phys. Chem. B* **2012**, *116*, 9676−9682.
(38) Chatgilialoglu, C.; Ferreri, C.; Terzidis, M. A. Purine 5′,8-Cyclonucleoside Lesions: Chemistry and Biology. *Chem. Soc. Rev.* **2011**, *40*, 1368−1382.
(39) Becke, A. D. Density-Functional Exchange-Energy Approximation with Correct Asymptotic Behavior. *Phys. Rev. A* **1988**, *38*, 3098−3100. Becke, A. D. Density-Functional Thermochemistry. III. The Role of Exact Exchange. *J. Chem. Phys.* **1993**, *98*, 5648−5652. Lee, C.; Yang, W.; Parr, R. G. Development of the Colle−Salvetti Correlation-Energy Formula into a Functional of the Electron Density. *Phys. Rev. B* **1988**, *37*, 785−789.
(40) Ditchfield, R.; Hehre, W. J.; Pople, J. A. Self-Consistent Molecular-Orbital Methods. IX. An Extended Gaussian-Type Basis for Molecular-Orbital Studies of Organic Molecules. *J. Chem. Phys.* **1971**, *54*, 724−728. Hehre, W. J.; Ditchfield, R.; Pople, J. A. Self-Consistent Molecular Orbital Methods. XII. Further Extensions of Gaussian-Type Basis Sets for Use in Molecular Orbital Studies of Organic Molecules. *J. Chem. Phys.* **1972**, *56*, 2257−2261.
(41) Miertuš, S.; Scrocco, E.; Tomasi, J. Electrostatic Interaction of a Solute with a Continuum. A Direct Utilization of ab Initio Molecular Potentials for the Prevision of Solvent Effects. *Chem. Phys.* **1981**, *55*, 117−129. Miertuš, S.; Tomasi, J. Approximate Evaluations of the Electrostatic Free Energy and Internal Energy Changes in Solution Processes. *Chem. Phys.* **1982**, *65*, 239−245. Cossi, M.; Barone, V.; Cammi, R.; Tomasi, J. Ab Initio Study of Solvated Molecules: A New Implementation of the Polarizable Continuum Model. *Chem. Phys. Lett.* **1996**, *255*, 327−335.
(42) Wong, M. H.; Wiberg, K. B.; Frisch, M. Hartree−Fock Second Derivatives and Electric Field Properties in a Solvent Reaction Field: Theory and Application. *J. Chem. Phys.* **1991**, *95*, 8991−8998.
(43) Frisch, M. J.; et al.et al. *Gaussian 09*, revision A.02; Gaussian Inc.: Pittsburgh, PA, 2009.
(44) Dennington, R.; Keith, T.; Millam, J. *GaussView*, version 5; Semichem Inc.: Shawnee Mission, KS, 2009.
(45) Narayana, N.; Weiss, M. A. Crystallographic Analysis of a Sex-Specific Enhancer Element: Sequence-Dependent DNA Structure, Hydration, and Dynamics. *J. Mol. Biol.* **2009**, *385*, 469−490.
(46) Gu, J.; Xie, Y.; Schaefer, H. F., III. Near 0 eV Electrons Attach to Nucleotides. *J. Am. Chem. Soc.* **2006**, *128*, 1250−1252.
(47) Gu, J.; Xie, Y.; Schaefer, H. F., III. Electron Attachment to Nucleotides in Aqueous Solution. *ChemPhysChem* **2006**, *7*, 1885−1887.
(48) Siefermann, K. R.; Liu, Y.; Lugovoy, E.; Link, O.; Faubel, M.; Buck, U.; Winter, B.; Abel, B. Binding Energies, Lifetimes and Implications of Bulk and Interface Solvated Electrons in Water. *Nat. Chem.* **2010**, *2*, 274−279.
(49) Pogozelski, W. K.; Tullius, T. D. Oxidative Strand Scission of Nucleic Acids: Routes Initiated by Hydrogen Abstraction from the Sugar Moiety. *Chem. Rev.* **1998**, *98*, 1089−1107.
(50) Chatgilialoglu, C.; Duca, M.; Ferreri, C.; Guerra, M.; Ioele, M.; Mulazzani, Q. G.; Strittmatter, H.; Giese, B. Selective Generation and Reactivity of 5′-Adenosinyl and 2′-Adenosinyl Radicals. *Chem.—Eur. J.* **2004**, *10*, 1249−1255.
(51) Sugiyama, H.; Tsutsumi, Y.; Fujimoto, K.; Saito, I. Photoinduced Deoxyribose C2′ Oxidation in DNA. Alkali-Dependent Cleavage of Erythrose-Containing Sites via a Retroaldol Reaction. *J. Am. Chem. Soc.* **1993**, *115*, 4443−4448.
(52) Zheng, Y.; Cloutier, P.; Hunting, D. J.; Sanche, L.; Wagner, J. R. Chemical Basis of DNA Sugar-Phosphate Cleavage by Low-Energy Electrons. *J. Am. Chem. Soc.* **2005**, *127*, 16592−16598.
(53) Zheng, Y.; Cloutier, P.; Hunting, D. J.; Wagner, J. R.; Sanche, L. Phosphodiester and *N*-Glycosidic Bond Cleavage in DNA Induced by 4−15 eV Electrons. *J. Chem. Phys.* **2006**, *124*, 064710.
(54) Rak, J.; Kobyłecka, M.; Storoniak, P. Single Strand Break in DNA Coupled to the O−P Bond Cleavage. A Computational Study. *J. Phys. Chem. B* **2011**, *115*, 1911−1917.